

Pilot Pattern Adaptation for 5G MU-MIMO Wireless Communications

Nassar Ksairi, Beatrice Tomasi, and Stefano Tomasin
Mathematical and Algorithmic Sciences Lab, France Research Center,
Huawei Technologies Co. Ltd., Boulogne-Billancourt, France.
Emails: {nassar.ksairi, beatrice.tomasi, stefano.tomasin}@huawei.com,

Abstract—To meet the goal of ten-fold increase in spectral efficiency, multiuser multiple-input-multiple-output (MU-MIMO) techniques capable of achieving high spatial multiplexing gains are expected to be an essential component of fifth-generation (5G) radio access systems. This increase in multiplexing gain, made possible by equipping base stations with a large number of antennas, entails a proportional increase in channel state information (CSI) acquisition overhead. This article addresses the problem of reducing this CSI overhead by optimizing the amount of time-frequency resources allocated for channel training purposes while not affecting the quality of the associated channel estimate. First we show that in MU-MIMO, adapting pilot symbol density in the time-frequency grid should be performed both on a per resource block (RB) basis and on the basis of groups of users sharing similar channel conditions. Next, we propose a practical scheme that can perform grouping based per-RB pilot pattern adaptation. Finally, we evaluate using both analytical and numerical results the gain in spectral efficiency that can be achieved using this scheme as compared to conventional MU-MIMO systems that use fixed pilot patterns.

I. INTRODUCTION

In contrast to existing wireless systems, next-generation MU-MIMO will most probably be deployed using base stations (BS) that are equipped with a large number of antennas thus increasing the system spectral efficiency. However, achieving this increase in spectral efficiency is conditioned on the availability of precise estimates of the channels between the different users and the BS [1]. CSI is typically obtained by sending reference signals (RS), also called pilots, which are known at both transmitter and receiver sides. The portion of time and frequency resources reserved to these training sequences is what constitutes the channel training overhead. In an uplink scenario where multiple users are simultaneously transmitting to the BS, the channel training overhead typically grows with the number of these users. This also applies to downlink user-specific pilots transmitted by the BS¹. There is thus a crucial need to compensate this increase in overhead. Whether in the uplink or in the downlink, special care should be paid so that the pilot signals of users scheduled at the same time-frequency resources are (at least partially) orthogonal to each other and that the symbol positions used by one of

them for pilot transmission are not used by another for data transmission to avoid data-pilot interference.

The issue of reducing channel training overhead in MU-MIMO was addressed in [2] and [3] where the authors propose to exploit the spatial correlation of users' channels to the BS antenna array in order to minimize the length of their training sequences. The proposed schemes rely on the fact that users' pilot signals can be separated to some extent at the BS through their spatial signature, provided that their low-rank channel covariance matrices are known.

Another promising approach to reduce channel training overhead without the additional overhead needed for spatial covariance estimation consists in reducing the *average* density of pilot symbols. Indeed, in wireless systems that use orthogonal frequency division multiplexing (OFDM), channel training is done by sending pilots on some predefined positions, i.e. according to a predefined *pilot pattern*, in the time-frequency resource grid. Once an estimate of the channel at the pilot positions is available, interpolation techniques are used to exploit correlation in time and frequency, and obtain the estimate of the channel on the grid positions carrying data. In principle, the required density of pilot symbols in a pilot pattern is related to the level of correlation of the channel coefficients along the time and the frequency axes. For instance, for users with a fast changing channel, density along the time axis must be increased with respect to (w.r.t.) almost-static users. On the other hand, a higher frequency selectivity requires denser pilots along the frequency axis. Adapting the pilot patterns to users' second-order statistics makes it possible to send/receive training sequences with different pilot symbol densities: some of these can be lower than the highest pilot density designed to cope with the worst-case channel. In [4], methods for choosing the pilot pattern for OFDM based on the channel time and frequency correlation properties are proposed. A method for selecting MIMO OFDM pilot patterns based on the channel signal-to-noise ratio (SNR), maximum Doppler frequency and root mean square delay spread is proposed in [5]. In [6], adaptive pilot patterns are proposed but the adaptation is done only w.r.t. users' quality-of-service (QoS) requirements. A method to assign OFDMA pilot patterns on the basis of groups of mobile users having the same speed is proposed in [7]. However, in this method groups with different pilot patterns are forced to occupy disjoint time intervals. All these works do not address the more challenging issue of pilot pattern

¹As opposed to cell-specific reference signals, user-specific pilots are transmitted only on the RBs on which the intended user is scheduled and they pass through the same MIMO precoding applied to the data symbols.

adaptation for MU-MIMO systems where the pilot symbols of different users could overlap due to spatial multiplexing.

Contributions

We propose a pilot pattern adaptation scheme that can lower pilot and signaling overhead for both uplink and downlink user-specific training sequences in MU-MIMO systems. The scheme consists in constraining the scheduler to group users based on their channels second-order statistics. Therefore, patterns with a reduced overhead can be used on a RB in which all scheduled users have milder requirements on pilots. Even though the scheme constrains the scheduler with the grouping step, we prove that the average spectral efficiency achieved with the proposed scheme is guaranteed to be larger than that of conventional pilot selection combined with any user scheduling paradigm, provided that the number of BS antennas and of cell users is large enough. Finally, we show through simulations that this property is valid even with practical values of the number of BS antennas and of cell users.

II. SYSTEM MODEL

We consider an OFDM-based MU-MIMO single-cell system where the BS is equipped with $M \gg 1$ antennas and assume that the OFDM resource grid is divided into $N_{\text{RB}} > 1$ RBs, each composed of N_s OFDM symbols, each comprising N_{SC} subcarriers (SCs), resulting in a total of $N_{\text{RE}} = N_s \times N_{\text{SC}}$ resource elements (REs) per RB. We denote the set of (single-antenna) terminals asking to be served as \mathcal{K} and define $K \stackrel{\text{def}}{=} |\mathcal{K}|$. Let us focus on RB r ($r \in \{1 \dots N_{\text{RB}}\}$) and let $\mathcal{U}_r^{\text{UL}} \subset \mathcal{K}$ (resp. $\mathcal{U}_r^{\text{DL}}$) designate the set of users assigned to this RB for uplink (resp. downlink) transmission such that

$$\max_{r \in \{1 \dots N_{\text{RB}}\}} \{|\mathcal{U}_r^{\text{UL}}|, |\mathcal{U}_r^{\text{DL}}|\} \leq U^{\text{mux}}, \quad (1)$$

where U^{mux} is the maximum spatial multiplexing gain allowed by the system. Define \mathcal{D}^{UL} and \mathcal{D}^{DL} as the subsets of $\{1 \dots N_s\} \times \{1 \dots N_{\text{SC}}\}$ that are used for uplink and downlink data transmission, respectively. Similarly, define \mathcal{P}^{UL} and \mathcal{P}^{DL} as the associated subsets of REs used for pilot transmission. The division of the set of REs in one RB into \mathcal{D}^{UL} and \mathcal{P}^{UL} (or into \mathcal{D}^{DL} and \mathcal{P}^{DL}) is typically dictated by the so-called *pilot pattern* defined by the communications standard. Finally, denote by $\mathbf{h}_{k,r,t,n}^{\text{UL}}$ and $\mathbf{h}_{k,r,t,n}^{\text{DL}}$ the vector of small-scale fading coefficients at subcarrier n ($n \in \{1 \dots N_{\text{SC}}\}$) during the t -th OFDM symbol ($t \in \{1 \dots N_s\}$) from user $k \in \mathcal{K}$ to the M antenna elements at the BS and from these antennas to user k , respectively. The samples $\mathbf{y}_{r,t,n}$ and $y_{k,r,t,n}$ received respectively at the BS and by user k are given by

$$\mathbf{y}_{r,t,n} = \sum_{k \in \mathcal{U}_r^{\text{UL}}} \sqrt{\eta_k P^{\text{UL}}} \mathbf{h}_{k,r,t,n}^{\text{UL}} x_{k,r,t,n} + \mathbf{v}_{r,t,n}, \quad (2)$$

$$y_{k,r,t,n} = \sqrt{\eta_k P^{\text{DL}}} (\mathbf{h}_{k,r,t,n}^{\text{DL}})^{\text{T}} \mathbf{x}_{r,t,n} + v_{k,r,t,n}, \quad (3)$$

where $\mathbf{v}_{r,t,n}$ and $v_{k,r,t,n}$ are independent identically-distributed (i.i.d.) $\mathcal{CN}(0, \sigma^2)$ noise samples, η_k is the large-scale fading factor, P^{UL} is the users' transmit power and P^{DL} is the transmit power of the BS. As for $x_{k,r,t,n}$ and

$\mathbf{x}_{r,t,n}$, they are zero-mean unit-power symbols sent by user k and the BS, respectively. In the sequel, we use the notations $\{s_{k,r,t,n}\}_{(t,n) \in \mathcal{D}}$ and $\{p_{k,r,t,n}\}_{(t,n) \in \mathcal{P}}$ to designate respectively the set of data symbols and of pilot symbols in RB r :

$$\forall k \in \mathcal{U}_r^{\text{UL}}, x_{k,r,t,n} = \begin{cases} s_{k,r,t,n}, & (t,n) \in \mathcal{D}^{\text{UL}}, \\ p_{k,r,t,n}, & (t,n) \in \mathcal{P}^{\text{UL}}. \end{cases} \quad (4)$$

In the uplink, we assume that *linear combining* is used to detect users' signals based on the samples $\frac{1}{M} (\mathbf{w}_{k,r,t,n}^{\text{UL}})^{\text{H}} \mathbf{y}_{r,t,n}$, where $\mathbf{w}_{k,r,t,n}^{\text{UL}}$ is the combining vector for user $k \in \mathcal{U}_r^{\text{UL}}$. These combining vectors are typically chosen depending on $\mathcal{U}_r^{\text{UL}}$ through some optimality criteria such as maximum-ratio combining (MRC) and zero-forcing (ZF) combining. Similarly, we assume that the BS applies *linear precoding* in the downlink so that

$$\mathbf{x}_{r,t,n} = \begin{cases} \sum_{k \in \mathcal{U}_r^{\text{DL}}} \frac{1}{M} \mathbf{w}_{k,r,t,n}^{\text{DL}} s_{k,r,t,n}, & (t,n) \in \mathcal{D}^{\text{DL}}, \\ \sum_{k \in \mathcal{U}_r^{\text{DL}}} \frac{1}{M} \mathbf{w}_{k,r,t,n}^{\text{DL}} p_{k,r,t,n}, & (t,n) \in \mathcal{P}^{\text{DL}}, \end{cases} \quad (5)$$

where $\mathbf{w}_{k,r,t,n}^{\text{DL}}$ is the precoding vector assigned to user $k \in \mathcal{U}_r^{\text{DL}}$ and normalized in accordance with P^{DL} . Here, $p_{k,r,t,n}$ is a *user-specific* pilot symbol that undergoes the same precoding as the data symbol $s_{k,r,t,n}$ and which is intended for the estimation of the effective channel $\frac{1}{M} (\mathbf{h}_{k,r,t,n}^{\text{DL}})^{\text{T}} \mathbf{w}_{k,r,t,n}^{\text{DL}}$ at the user terminal. Vectors $\mathbf{w}_{k,r,t,n}^{\text{DL}}$ are typically based on $\mathcal{U}_r^{\text{DL}}$ using some optimality criteria, e.g. maximum-ratio transmission (MRT) and zero-forcing (ZF) precoding.

Each entry of $\mathbf{h}_{k,r,t,n}^{\text{UL}}$ and $\mathbf{h}_{k,r,t,n}^{\text{DL}}$ is assumed to be a two-dimensional wide-sense stationary (WSS) random process that is band limited [9] w.r.t. both t and n . In other words, the Fourier transform of both its t -axis and its n -axis auto-correlation functions has a finite support. The highest value in the frequency domain support is the maximum Doppler frequency shift denoted as f_k^D , while the largest value in the time domain support is the maximum delay spread denoted as τ_k^{max} . We assume that $\forall k \in \mathcal{K}$, the pair $(\tau_k^{\text{max}}, f_k^D)$ can take only a finite number $G > 1$ of values denoted as $\{(\tau_g, f_g)\}_{1 \leq g \leq G}$. In practice, this assumption amounts to quantizing the different values of $(\tau_k^{\text{max}}, f_k^D)$. The set of users whose channels follows the g -th model are denoted as \mathcal{G}_g , where

$$\mathcal{G}_g \stackrel{\text{def}}{=} \{k \in \mathcal{K} | (\tau_k^{\text{max}}, f_k^D) = (\tau_g, f_g)\}, 1 \leq g \leq G. \quad (6)$$

As in [9], we assume that one can get small-enough² channel estimate mean-square error (MSE) by restricting \mathcal{P}^{UL} and \mathcal{P}^{DL} to be composed of regularly spaced positions with a pilot symbol density two-times the density dictated by the *sampling theorem for band limited WSS random processes*. This rule of thumb implies that the *maximum* pilot symbol spacing that can be used on a channel g is Δ_g^s OFDM symbols in the time domain and Δ_g^{SC} SCs in the frequency domain, where

$$\Delta_g^s \stackrel{\text{def}}{=} \left\lfloor \frac{1}{4f_g T_s} \right\rfloor, \quad \Delta_g^{\text{SC}} \stackrel{\text{def}}{=} \left\lfloor \frac{1}{4\tau_g \Delta f} \right\rfloor. \quad (7)$$

²In the sense that the associated channel estimation MSE does not exceed a predefined target value.

Here, T_s denotes the duration of the OFDM symbol and Δf the inter-subcarrier frequency separation.

III. CONVENTIONAL MU-MIMO PILOT PATTERNS

In current wireless systems, the same pilot pattern, denoted as $\mathcal{P}^{\text{conv,UL}}$ (conv stands for ‘conventional’), is used on all uplink RBs while the same pilot pattern, denoted as $\mathcal{P}^{\text{conv,DL}}$, is used on all downlink RBs. Both $\mathcal{P}^{\text{conv,UL}}$ and $\mathcal{P}^{\text{conv,DL}}$ are designed to cope with the worst-case scenario in which $\forall r, g, \mathcal{U}_r^{\text{UL}} \cap \mathcal{G}_g \neq \emptyset$ and $\mathcal{U}_r^{\text{DL}} \cap \mathcal{G}_g \neq \emptyset$. Combining this with the requirement that the total number of pilot symbols in a RB should be an integer multiple of the number of multiplexed users, we get

$$|\mathcal{P}^{\text{conv,UL}}| = |\mathcal{P}^{\text{conv,DL}}| = \max_{g \in \{1 \dots G\}} \left\lceil \frac{N_s}{\Delta_g^s} \right\rceil \left\lceil \frac{N_{\text{SC}}}{\Delta_g^{\text{SC}}} \right\rceil U^{\text{mux}} \quad (8)$$

Plugging $U^{\text{mux}} = 4$ and the LTE system parameters into (8) while assuming a worst-case Doppler frequency shift $f^D = 300$ Hz and maximum delay spread $\tau^{\text{max}} = 4.69$ ms yields $|\mathcal{P}^{\text{conv}}| = 24$, in agreement with the uplink and downlink pilot patterns of LTE-Advanced shown in Fig. 1.

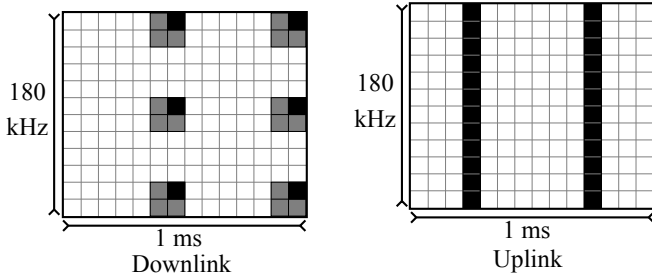


Fig. 1. Pilot pattern for 4-layer user-specific RS in LTE-Advanced

The average spectral efficiency R_r of RB r on which the subset \mathcal{U}_r of users is scheduled with pilot pattern \mathcal{P}_r is

$$R_r(\mathcal{U}_r, \mathcal{P}_r) \stackrel{\text{def}}{=} \frac{1}{N_{\text{RE}}} \sum_{k \in \mathcal{U}_r} \sum_{(t,n) \notin \mathcal{P}_r} \log(1 + \text{SINR}_{k,r,t,n}) \quad (9)$$

where \log is the base-2 logarithm and where $\text{SINR}_{k,r,t,n}$ is user k signal-to-interference-plus-noise ratio on (r, t, n) that is given by $\text{SINR}_{k,r,t,n} = \text{SINR}_{k,r,t,n}^{\text{UL}}$ in the uplink and by $\text{SINR}_{k,r,t,n} = \text{SINR}_{k,r,t,n}^{\text{DL}}$ in the downlink. Here, we defined

$$\text{SINR}_{k,r,t,n}^{\text{UL}} \stackrel{\text{def}}{=} \frac{\eta_k P^{\text{UL}} |\mathbf{w}_{k,r,t,n}^{\text{H}} \mathbf{h}_{k,r,t,n}|^2}{\sum_{j \neq k} \eta_j P^{\text{UL}} |\mathbf{w}_{k,r,t,n}^{\text{H}} \mathbf{h}_{j,r,t,n}|^2 + \mathbf{w}_{k,r,t,n}^{\text{H}} \mathbf{w}_{k,r,t,n} \sigma^2} \quad (10)$$

and

$$\text{SINR}_{k,r,t,n}^{\text{DL}} \stackrel{\text{def}}{=} \frac{\eta_k P^{\text{DL}} |\mathbf{w}_{k,r,t,n}^{\text{H}} \mathbf{h}_{k,r,t,n}|^2}{\sum_{j \neq k} \eta_j P^{\text{DL}} |\mathbf{w}_{j,r,t,n}^{\text{H}} \mathbf{h}_{k,r,t,n}|^2 + M^2 \sigma^2} \quad (11)$$

The associated maximum spectral efficiency is given by

$$R^{\text{conv}} \stackrel{\text{def}}{=} \max_{\{\mathcal{U}_r\}_{r \in \{1 \dots N_{\text{RB}}\}}} \frac{1}{N_{\text{RB}}} \sum_{r=1}^{N_{\text{RB}}} R_r(\mathcal{U}_r, \mathcal{P}^{\text{conv}}). \quad (12)$$

Solving (12) involves high CSI acquisition overhead needed to have CSI at the BS about each user’s channel on all the RBs. Many of the existing user scheduling paradigms try to find the RB allocation that solves (exactly or approximately) (12). Finding such RB allocation is out of the scope of this work. However, we evaluate how the proposed pilot allocation and grouping affect the maximum spectral efficiency of the system.

For the sake of notational simplicity, we drop from now on the use of superscripts DL and UL. For instance, the notations $\mathcal{U}_r^{\text{UL}}$ and $\mathcal{U}_r^{\text{DL}}$ are merged into \mathcal{U}_r while $\mathcal{P}^{\text{conv,UL}}$ and $\mathcal{P}^{\text{conv,DL}}$ are replaced with $\mathcal{P}^{\text{conv}}$. Whenever needed, the transmission scenario, whether downlink or uplink, will be explicitly mentioned.

IV. ADAPTIVE PILOT PATTERN SELECTION AND USER GROUPING FOR MU-MIMO

Using the pilot patterns of Section III for user-specific RS in 5G systems would be very inefficient. Indeed, in these systems: *i*) users’ channel conditions in one cell can be very diverse due to their larger numbers, and *ii*) longer pilot sequences are needed because more users are spatially multiplexed. For example, a MU-MIMO transmission to 8 users would require 48 pilot symbols per RB as opposed to 24 in the case of 4 multiplexed users. We thus propose an *adaptive* pilot pattern selection that is based on the following guidelines.

A. Guidelines

Let $\mathcal{R} \subset 2^{\{1 \dots N_s\}} \times \{1 \dots N_{\text{SC}}\}$ designate the predefined set of possible values of \mathcal{P} and assume that any $\mathcal{P} \in \mathcal{R}$ has a regular pilot symbol spacing denoted as $(\delta_{\mathcal{P}}^s, \delta_{\mathcal{P}}^{\text{SC}})$ which satisfies

$$\forall \mathcal{P}, \mathcal{Q} \in \mathcal{R} \text{ s.t. } \mathcal{P} \neq \mathcal{Q}, (\delta_{\mathcal{P}}^s, \delta_{\mathcal{P}}^{\text{SC}}) \neq (\delta_{\mathcal{Q}}^s, \delta_{\mathcal{Q}}^{\text{SC}}). \quad (13)$$

The constraint in (13) means that for two pilot patterns to be considered as distinct they should have different pilot symbol spacing values, either on the time axis or on the frequency axis or on both. It is also natural to bound the number of possible pilot patterns with the number G of distinct statistical channel conditions:

$$N_{\mathcal{R}} \stackrel{\text{def}}{=} |\mathcal{R}| \leq G. \quad (14)$$

This paper focuses on the practical case where channel spatial covariance matrices are not known at the BS and where, consequently, the training sequence shortening techniques of [2] or [3] do not apply. We thus impose that,

$$\forall \mathcal{P} \in \mathcal{R}, |\mathcal{P}| = \left\lceil \frac{N_s}{\delta_{\mathcal{P}}^s} \right\rceil \left\lceil \frac{N_{\text{SC}}}{\delta_{\mathcal{P}}^{\text{SC}}} \right\rceil U^{\text{mux}}. \quad (15)$$

Figure 2 shows $N_{\mathcal{R}} = 4$ pilot patterns which satisfy conditions (13)–(15) for a system with $G \geq 4$ and $U^{\text{mux}} = 4$. In the following, we assume that such patterns can be used for both uplink and downlink pilot transmissions.

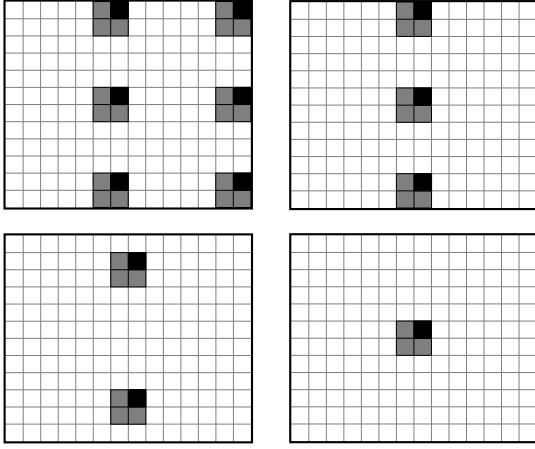


Fig. 2. Example of adaptive pilot patterns for 4-layer user-specific RS.

We use the term *pilot pattern adaptation* to designate any mapping \mathcal{P}_r from $\{1 \cdots N_{\text{RB}}\} \times 2^{\mathcal{K}}$ to \mathcal{R} where \mathcal{R} satisfies conditions (13), (14) and (15). Any such mapping assigns to each RB r used by a set \mathcal{U}_r of users a set of pilot positions $\mathcal{P}_r(\mathcal{U}_r)$ indicated as \mathcal{P}_r . In other words, pilot pattern adaptation is performed on a per-RB basis so that all users scheduled in the same RB have the same pilot pattern, thus avoiding interference between data and pilot symbols. Moreover, the pilot pattern on any RB should accommodate the user with the worst-case statistical channel conditions scheduled in that RB, i.e. $\forall r \in \{1 \cdots N_{\text{RB}}\}$,

$$\begin{aligned} \delta_{\mathcal{P}_r}^{\text{SC}} &\leq \min \{ \Delta_g^{\text{SC}} | g \in \{1 \cdots G\}, \mathcal{G}_g \cap \mathcal{U}_r \neq \emptyset \}, \\ \delta_{\mathcal{P}_r}^s &\leq \min \{ \Delta_g^s | g \in \{1 \cdots G\}, \mathcal{G}_g \cap \mathcal{U}_r \neq \emptyset \}. \end{aligned} \quad (16)$$

Finally, scheduling should take into account users' pilot density requirements, which implies the need for an additional process that identifies the groups $\mathcal{G}_1, \dots, \mathcal{G}_G$ and which interacts with the scheduling process, i.e.

$$\forall r \in \{1 \cdots N_{\text{RB}}\}, \mathcal{U}_r = \mathcal{U}_r(\mathcal{G}_1, \dots, \mathcal{G}_G). \quad (17)$$

We propose a method that performs both pilot pattern adaptation and user scheduling following the guidelines in (13)–(17).

Remark 1. *In order to perform pilot pattern adaptation and user scheduling following the guidelines in (13)–(17) it is necessary that the values of f_g and τ_g for $g = 1, \dots, G$ are available at the BS. Interestingly, acquiring these values can be achieved without additional overhead. Indeed, variation over time of the maximum Doppler frequency shift and the maximum delay spread of a channel is typically much slower than the variations of the channel coefficients. These parameters can thus be estimated based on previous uplink pilot transmissions.*

B. Grouping Based Pilot Pattern Adaptation and Scheduling

The proposed scheme consists in first pre-assigning the RBs to the groups $\mathcal{G}_1, \dots, \mathcal{G}_G$ using a mapping $g_r : \{1 \cdots N_{\text{RB}}\} \rightarrow$

$\{1 \cdots G\}$. This mapping could be the outcome of optimizing RB allocation to the pilot pattern groups based on average per-RB channel quality indicators. Otherwise, g_r could be a *fixed* pre-assignment of RBs. One example of such mapping is the one adopted in Algorithm 1 and which satisfies $\forall g \in \{1 \cdots G\}, |\{r | g_r = g\}| / N_{\text{RB}} \approx |\mathcal{G}_g| / K$ to guarantee fairness among the different groups.

Once this pre-assignment is done, the per-RB pilot pattern adaptation consists in choosing the pilot pattern $\mathcal{P}(\mathcal{G}_{g_r})$ that has the largest pilot inter symbol distances $\delta_{\mathcal{P}}^{\text{SC}}$ and $\delta_{\mathcal{P}}^s$ satisfying the condition in (16). Then, the scheduler chooses $\mathcal{U}_r \subset \mathcal{G}_{g_r}$. The asymptotic results given below are valid for

Algorithm 1 Grouping Based Pilot Pattern Adaptation and User Scheduling (with fixed RB pre-assignment)

```

for  $g \in \{1 \cdots G\}$  do
  for  $r \in \left\{ \left\lceil \frac{N_{\text{RB}} |\cup_{h=1}^{g-1} \mathcal{G}_h|}{K} \right\rceil + 1, \dots, \left\lceil \frac{N_{\text{RB}} |\cup_{h=1}^g \mathcal{G}_h|}{K} \right\rceil \right\}$  do
     $\mathcal{P}_r \leftarrow \mathcal{P}(\mathcal{G}_g)$ 
     $\mathcal{U}_r \leftarrow \mathcal{U} \subset \mathcal{G}_g$ 
  end for
end for

```

arbitrary \mathcal{U}_r including those obtained by applying state-of-the-art scheduling paradigms to \mathcal{G}_{g_r} and those obtained by random selection of \mathcal{U}_r from within \mathcal{G}_{g_r} .

Remark 2. *Because of the grouping step and the possibility of arbitrarily choosing $\mathcal{U}_r \subset \mathcal{G}_{g_r}$, Algorithm 1 is much less demanding in both computational complexity and CSI acquisition overhead than any conventional scheme that tries to solve (12). Furthermore, we show that Algorithm 1 outperforms any conventional scheme that uses fixed pilot pattern assignment, at least for large-enough numbers of users and BS antennas. As for the signaling overhead needed to inform a user of the selected pilot pattern, it is of the order of $\log G$ which is typically very small, e.g. only 2 bits are needed when $G = 4$.*

We focus on the case where perfect CSI³ is available at the BS and where the combining coefficients $\mathbf{w}_{k,r,t,n}^{\text{UL}}$ are chosen based on the MRC criterion and the precoding coefficients $\mathbf{w}_{k,r,t,n}^{\text{DL}}$ based on the MRT criterion. In this case, let $R_r^{\text{grp}} \stackrel{\text{def}}{=} \frac{1}{N_{\text{RB}}} \sum_{r=1}^{N_{\text{RB}}} R_r(\mathcal{U}_r, \mathcal{P}(\mathcal{G}_{g_r}))$ be the spectral efficiency achieved by Algorithm 1, where $R_r(\cdot, \cdot)$ is given by (9) and where grp stands for ‘grouping’. The following theorem states that Algorithm 1 asymptotically outperforms any conventional pilot pattern selection and user scheduling in terms of average spectral efficiency for a sufficiently large number of antennas at the BS and of users in the cell.

Theorem 1. *Assume that $\forall r$, the empirical distribution of the large-scale fading coefficients $\{\eta_k\}_{k \in \mathcal{U}_r}$ converges as $U^{\text{mux}} \rightarrow \infty$ to the distribution of a random variable η with mean $\bar{\eta}$.*

³In practice, this case amounts to assuming that the MSE of uplink channel estimation is negligible and that channel aging is *not* an issue for downlink transmission. Similar results can be obtained in the case of imperfect CSI and/or for other combining and precoding criteria but are not included.

Then as $M, U^{\text{mux}}, N_{\text{RE}}, |\mathcal{G}_g| \rightarrow \infty$ such that $U^{\text{mux}}/M \rightarrow \alpha$, $U^{\text{mux}}/N_{\text{RE}} \rightarrow \beta$, $|\mathcal{G}_g|/K \rightarrow \gamma_g$ where α, β, γ_g are constants,

$$\lim_{M, U^{\text{mux}} \rightarrow \infty} \mathbb{P} \{R^{\text{grp}} > R^{\text{conv}}\} = 1. \quad (18)$$

We let N_{RE} (which is fixed in practice) grow with U^{mux} only to get nontrivial asymptotic expressions since $|\mathcal{P}(\mathcal{G}_g)|$ also grows with U^{mux} due to (15). The assumption about the empirical distribution of $\{\eta_k\}_{k \in \mathcal{U}_r}$ for all r is also technical and is in practice satisfied in any cell with a sufficiently large number of users that are randomly distributed over the cell area. In this case, roughly speaking, even the baseline scheduler employing exhaustive search ends up assigning to each RB r a set \mathcal{U}_r of users which have diverse pathloss profiles, thus validating the assumption.

Proof. For given empirical values $\{\eta_k\}_{k \in \mathcal{K}}$, the tools of [10, Theorem 3] can be applied to $\text{SINR}_{k,r,t,n}$ defined by (10) and (11) to show that $\forall r, t, n, \mathcal{U}_r, \text{SINR}_{k,r,t,n} - \text{SINR}_{k,r,t,n}^{\text{det}} \xrightarrow{a.s.} 0$, where det stands for ‘deterministic equivalent’ and where

$$\text{SINR}_{k,r}^{\text{det}} = \begin{cases} \frac{\eta_k P^{\text{UL}}}{\sigma^2/M + (1/M) \sum_{j \in \mathcal{U}_r} \eta_j P^{\text{UL}}}, & \text{in the uplink,} \\ \frac{\eta_k P^{\text{DL}}}{\sigma^2/M + (U^{\text{mux}}/M) \eta_k P^{\text{DL}}}, & \text{in the downlink.} \end{cases} \quad (19)$$

Next, by our assumption about the empirical distribution of η_k , we can apply the continuous-mapping theorem along with standard convergence arguments to show after some tedious, but rather straightforward, steps that (9) and (19) lead to

$$\frac{R^{\text{grp}}}{U^{\text{mux}}} - \sum_{g=1}^G \frac{|\mathcal{G}_g|}{K} \left(1 - \frac{|\mathcal{P}(\mathcal{G}_g)|}{N_{\text{RE}}}\right) \log(1 + \overline{\text{SINR}}) \xrightarrow{p} 0, \quad (20)$$

$$\frac{R^{\text{conv}}}{U^{\text{mux}}} - \left(1 - \frac{\max_g |\mathcal{P}(\mathcal{G}_g)|}{N_{\text{RE}}}\right) \log(1 + \overline{\text{SINR}}) \xrightarrow{p} 0, \quad (21)$$

where

$$\overline{\text{SINR}} \stackrel{\text{def}}{=} \begin{cases} 2^{\mathbb{E}_\eta \left[\log \left(1 + \frac{\eta P^{\text{UL}}}{\sigma^2/M + (U^{\text{mux}}/M) \eta P^{\text{UL}}} \right) \right]} - 1, & \text{in the uplink,} \\ 2^{\mathbb{E}_\eta \left[\log \left(1 + \frac{\eta P^{\text{DL}}}{\sigma^2/M + (U^{\text{mux}}/M) \eta P^{\text{DL}}} \right) \right]} - 1, & \text{in the downlink.} \end{cases} \quad (22)$$

Finally, since $\sum_{g=1}^G \frac{|\mathcal{G}_g|}{K} = 1$ and $\max_h |\mathcal{P}(\mathcal{G}_h)| \geq |\mathcal{P}(\mathcal{G}_g)| \forall g \in \{1 \dots G\}$, from (20) and (21) we get (18). \square

V. NUMERICAL RESULTS

We evaluate the spectral efficiency of the proposed pilot allocation scheme and we compare it to that obtained by conventional pilot allocation. The performance is computed assuming $N_{\text{RB}} = 4$ RBs, to each of which U^{mux} users are allocated from a total of $K = N_{\text{RB}} U^{\text{mux}}$ users. We let U^{mux} vary from 4 to 7. We consider $G = 4$ possible profiles of time-frequency second-order statistics characterizing the users’ channels. The values for the different Doppler frequencies and delay spreads are taken from [11] and are summarized in Table I. In the table, EPA stands for the ‘‘Extended Pedestrian

TABLE I
CHANNEL PARAMETERS FOR $G = 4$ GROUPS.

Group index g	Model Name	Doppler shift f_g (Hz)	Delay spread τ_g (μs)
1	EPA5	5	0.41
2	EVA70	70	2.51
3	ETU70	70	4.69
4	ETU300	300	4.69

A’’, EVA for the ‘‘Extended Vehicular A’’ and ETU for the ‘‘Extended Type Urban’’ channel models. Groups $\mathcal{G}_1, \mathcal{G}_2, \mathcal{G}_3$ and \mathcal{G}_4 , each of which composed of users that share the same channel profile, are assumed to all have the same size: $|\mathcal{G}_g| = K/G, \forall g = 1, 2, 3, 4$. Finally, $\forall k \in \mathcal{K}$, the SNR $\eta_k P^{\text{UL/DL}}/\sigma^2 = 10$ dB. At each random channel realization, the SINR is evaluated per user and per RE in each RB according to (10) and (11). When the conventional pilot pattern is used, the K users are scheduled to the 4 RBs based on (12). In order to do so, we perform an exhaustive search among all possible user allocation combinations and we choose the one that results in the highest spectral efficiency. Instead, when the proposed scheme is used, we only optimize the association of the G pilot pattern groups to the N_{RB} RBs.

Fig. 3 shows the average spectral efficiency obtained by the proposed scheme (black curves), and that for the conventional pilot allocation with exhaustive search scheduling (gray curves). These results are obtained by averaging over 10 channel realizations. In all configurations, the proposed scheme achieves a higher spectral efficiency, even for a moderate number of antennas at the BS, e.g. $M = 64$, and a moderate number of users per RB, e.g. $U^{\text{mux}} = 4$, and in spite of the fact that exhaustive search is performed when using the conventional scheme. This is due to the fact that, thanks to the asymptotic channel properties of large antenna arrays, the gain in spectral efficiency due to the increase in the number of summations in (9) with the proposed scheme, i.e. the increase in the average value of $\left(1 - \frac{|\mathcal{P}_r|}{N_{\text{RE}}}\right)$, outweighs any potential decrease in the term $\log(1 + \text{SINR}_{k,r,t,n})$ due to restricting the scheduler with the grouping step.

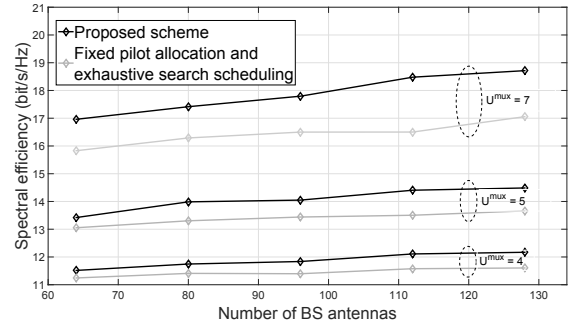


Fig. 3. Average spectral efficiency vs. M (SNR=10 dB).

Fig. 4 shows the relative gain in average spectral efficiency w.r.t. conventional pilot assignment with exhaustive search scheduling for different values of M and U^{mux} . The dashed

curve is the theoretical upper bound derived from (20) and (21). As expected, with larger values of M the gain gets closer to the asymptotic upper bound. For instance, at $U^{\text{mux}} = 7$ the relative gain increases from 7% to 12% when M increases from 64 to 112, thus getting closer to the 16% upper bound. This gain will be even larger when practical scheduling methods that are not based on exhaustive search are used as baseline.

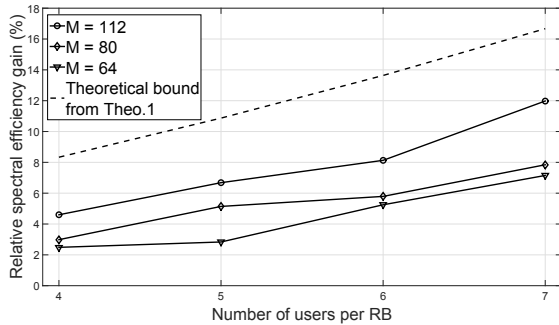


Fig. 4. Spectral efficiency gain vs. U^{mux} .

VI. CONCLUSION

In this paper, we presented a pilot pattern adaptation scheme for MU-MIMO that consists in grouping users based on their pilot density requirements. We further analytically proved that any state-of-the-art scheduling method when used along with fixed pilot pattern assignment will be outperformed by the proposed scheme in the limit of large numbers of users and BS antennas, provided that users are affected by sufficiently diverse channel conditions. We finally showed through simulations that this advantage holds even with moderate values of these parameters. Future research directions include proposing schemes capable of performing joint pilot pattern selection and user scheduling and studying the effect of pilot pattern adaptation on pilot contamination in multicell MU-MIMO scenarios.

REFERENCES

- [1] E. Björnson, E. G. Larsson, and T. L. Marzetta, "Massive MIMO: Ten Myths and One Critical Question," *IEEE Communications Magazine*, vol. 54, no. 2, pp. 114-123, February 2016.
- [2] B. Tomasi and M. Guillaud, *Pilot Length Optimization for Spatially Correlated Multi-User MIMO Channel Estimation*, in *Asilomar Conference on Signals, Systems and Computers*, Pacific Grove, CA, Nov. 2015.
- [3] A. Adhikary, J. Nam, J. Ahn, and G. Caire, "Joint Spatial Division and Multiplexing: The Large-Scale Array Regime," *IEEE Trans. Info. Theory*, vol. 59, no. 10, pp. 6441-6463, Oct. 2013.
- [4] J.-C. Guey, A. Osseiran, *Adaptive Pilot Allocation in Downlink OFDM*, in *WCNC*, Las Vegas, NV, Mar. 2008.
- [5] M. Simko, P. S. R. Diniz, and M. Rupp, *Design Requirements of Adaptive Pilot-Symbol Patterns*, in *ICC*, Budapest, June 2013.
- [6] O. Simeone and U. Spagnolini, *Adaptive Pilot Pattern for OFDM Systems*, in *ICC*, Paris, June 2004.
- [7] S. Lee, J. Y. Lee, and H. S. Lee, *Group-Based Pilot Design Method in Mobile OFDMA Systems*, in *ICACT*, Phoenix Park, Korea, Feb. 2008.
- [8] C. Lim, T. Yoo, B. Clerckx, B. Lee, and B. Shim, "Recent Trend of Multuser MIMO in LTE-Advanced," *IEEE Commun. Mag.*, vol. 51, no. 3, pp. 127-135, Mar. 2013.

- [9] P. Hoeher, S. Kaiser, and P. Robertson, *Two-Dimensional Pilot-Symbol-Aided Channel Estimation by Wiener Filtering*, in *ICCASP*, Munich, Apr. 1997.
- [10] J. Hoydis, S. t. Brink, M. Debbah, "Massive MIMO in the UL/DL of Cellular Networks: How Many Antennas Do We Need?" *IEEE J. Sel. Areas Commun.*, vol. 31, no. 2, pp. 160-171, Feb. 2013.
- [11] The 3rd Generation Partnership Project (3GPP), *Evolved Universal Terrestrial Radio Access (E-UTRA); Base Station (BS) radio transmission and reception*. Available: <http://www.3gpp.org/>, Sept. 2015.